USE OF MATHEMATICAL MODELING IN SELECTING A HEAT-TREATMENT REGIME

V. V. Kotov,[1,3] **K. I. Sergeeva,**[2,3]
V. A. Troyanov,[2,4] **and S. V. Belikov**[3]

Optimizing the processes used to make new and existing products is an important problem in modern industry. The urgency of this matter has led to broad use of mathematical modeling to model various industrial operations, including heat treatments. However, the adequacy of the results obtained by using the finite-elements method to model physical processes is still open to debate. The goal of this article is to evaluate results from mathematical modeling performed to choose regimes for the heat treatment of low-alloy steel and an aluminum alloy and compare those results with the results of a physical experiment.
Keywords: *modeling, steel, aluminum alloy, heat treatment, structure, properties, deformation.*

Heat treatment is one of the most important processes in the manufacture of different types of metal products. As part of the production process, heat treatment can either be an intermediate operation performed mainly to prepare a material for shaping or cutting or it can be a final operation needed to impart the necessary properties to the product [1]. The composition of the metal and the heat-treatment regime have a significant effect on the product's service life [2].

In designing heat-treatment regimes, the first priority is to obtain the service properties specified for products while also standardizing the regimes and ensuring that they are well-suited for industrial use. The goals here are to shorten the amount of time needed to make the new product, reduce the material and labor costs incurred in the production process, ensure that that process is very efficient, and improve the product's quality [2].

In connection with this, the use of mathematical modeling based on the finite-elements method is becoming increasingly popular in new-product development and introduction, as well as for eliminating the causes of product rejection during the manufacturing process. Modeling production processes makes it possible to more quickly obtain the properties desired for the product by optimizing the heat-treatment regime based on the results of calculations and making any necessary changes to the product's design with allowance for the calculated levels of stress and strain. It thus becomes possible to avoid having to perform physical experiments and make prototypes (or models) during the initial stages of the design and development of heat-treatment regimes. The result is a reduction in production costs, an improvement in product quality, and an increase in productivity.

The goal of the present study is to use mathematical modeling to select the heat-treatment regime for oil and gas industry piping made of low-alloy steels and to verify the results of calculations of the mechanical properties of aluminum alloys after heat treatment. Tubular semifinished products made for the petrochemical and gas industries will be used as an example.

---

[1] Representative of the ESI Group in the Russian Federation, Ekaterinburg, Russia; e-mail: viacheslav.kotov@esi-group.com.

[2] MECAS ESI s.r.o., Pilsen, Czech Republic; e-mail: ksenia.sergeeva@esi-group.com.

[3] Ural Federal University, Ekaterinburg, Russia; e-mail: srgbelikov@yandex.ru.

[4] Institute of Metal Physics, Ural Branch of the Russian Academy of Sciences, Ekaterinburg, Russia;
  e-mail: vsevolod.troyanov@esi-group.com.

The finite-elements method is currently widely employed as the foundation for modeling physical processes. However, in order to realistically model different stages of a production process, it is necessary to know the physical laws that describe the behavior of a material during heating, deformation, etc. This is the type of integrated approach to solving production problems that is used in the Visual Heat Treatment program developed by the company ESI Group. The program is designed to solve problems concerning the heat treatment of materials.

The program is based on the interaction of five modules: thermal and metallurgical analysis; electromagnetism; diffusion; the formation of secondary phases; analysis of mechanical properties. The different phase transformations in steels are calculated using the Kolmogorov–Johnson–Mehl–Avrami equation, the Koistinen–Marburger equation, the Leblon model, and thermokinetic and isothermal diagrams of the decomposition of supercooled austenite.

Work in Visual Heat Treatment begins with the construction of a grid of finite elements for the given product. Since the tube has symmetry, the plane of symmetry is specified relative to the Y-axis and calculations are performed for one-half of the product to reduce computing time. Fastening conditions were introduced for the Z and Y axes (Fig. 1a) to prevent undesirable displacements of the product during heat treatment.

The process of entering the theoretical parameters with the use of Heat Treatment Advisor is carried out in seven stages (Fig. 1b). The information that is entered includes the material, the temperature to which the product is heated, the medium, the cooling conditions, and the fastening of the product during heat treatment. Then Computation Manager is launched.

The materials chosen for study were low-alloy tube steel 20KhMF and aluminum alloy AD35. Steel 20MoCr4_022C and aluminum alloy AlMgSi were chosen from the database of the company ESI Group to perform calculations in Visual Heat Treatment. Steel 26Kh1MFA from the Severskii Pipe Plant was used to perform a heat treatment in a laboratory furnace and conduct subsequent mechanical tests. Tables 1 and 2 show the compositions of the materials used for the calculations and for the experiment.

In both cases, we modeled the heat treatment of a pipe with a diameter of 219 mm and a wall-thickness of 8 mm.

The parameters that were used to calculate the heat treatment of a pipe of steel 20MoC4_022C: quenching from $t = 890°C$ in a sprayer unit; quenching from $t = 890°C$ in oil; cooling in air from $t = 890°C$.

The heat treatment administered to steel 26Kh1MFA in order to perform mechanical tests: quenching from $t = 880°C$ in water; quenching from $t = 880°C$ in oil; cooling in air from $t = 880°C$.

The parameters that were used to calculate the heat treatment of the aluminum alloy pipe: annealing at $t = 370°C$; cooling in air.

The heat treatments that were performed for the metallographic studies and mechanical tests were conducted in SNOL laboratory furnaces.

A metallographic analysis was performed on an Epiphot-200 light microscope with a magnification ×(200–1000). Photographs of the microstructure were obtained using a Nikon digital camera and the program Nis-Elements Basic Research.

Vickers hardness was determined as part of the evaluation of the test steel's mechanical properties.

Modeling the quenching of the steel pipe in a sprayer and in oil and the steel's normalization yielded results on the distribution of the structural components over the cross section, the distortion of the pipe, residual stresses, and mechanical properties.

Figure 2 shows the microstructure of the pipe obtained from quenching it in the sprayer. The main structural component was martensite, the concentration of which was 96.5% on the surface and 90% at the center. There was also a small amount of bainite (3–8%) and residual austenite (roughly 0.3%).

In the case of quenching in oil, the calculations showed an increase in the content of bainite to 46% on the surface of the pipe and 54% at its center. The amount of residual austenite present was at the level 0.2%, while the remainder of the tube was composed of martensite.

After normalization, 59% of the steel was a ferrite-pearlite mixture, 34% was bainite, and 7% was martensite. There was very little residual austenite (0.05%).

Comparison of the results of calculation of the structural components in Visual Heat Treatment and the experimental data showed that they were very similar to one another. It can be seen from the thermokinetic diagram (TKD) of the decomposition of supercooled austenite in steel 26Kh1MFA (Fig. 3) that martensite is formed in the structure (Fig. 4a) dur-
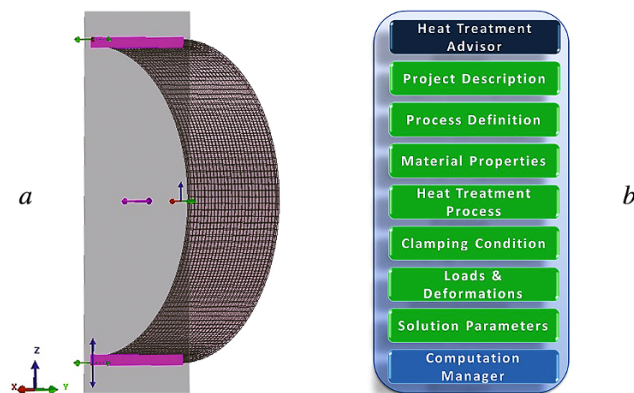
Fig. 1. Beginning work in the program Visual Heat Treatment: *a*) tube-fastening conditions; *b*) sections of Heat Treatment Advisor.
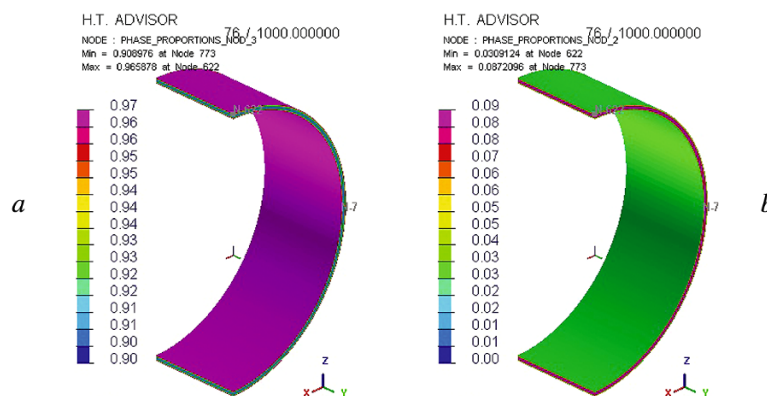

Fig. 2. Distribution of the structural components over the cross section of the pipe after quenching in a sprayer (calculation): *a*) martensite; *b*) bainite.

ing cooling at rates greater than 20°C/sec. There may also be a small amount of bainite, although optical microscopy can only identify the structural components which are present in concentrations greater than 5–10%.

The cooling rate in oil was on the order of 10°C/sec. As a result, quenching formed a heterogeneous martensite-bainite structure (Fig. 4*b*). This result was also seen in the calculations.

In accordance with the TKD, the bainite transformation in steel 26Kh1MFA takes place with relatively low cooling rates (about 0.2°C/sec). Thus, during normalization the austenite undergoes transformations of classes I, II, and III. The structure consists of uniformly distributed sections of a ferrite-pearlite mixture, bainite, and martensite (Fig. 4*c*).

One important stage in the modeling of heat-treatment processes is calculation of the mechanical properties and strains during heating and cooling, since maintaining the original geometry of the product, its dimensions, and the quality of its surface finish are key considerations in the actual heat treatment [2]. However, a number of factors, including high stresses, a change in the specific volume of the alloy during phase transformations, and certain features of the shape of the product can cause it to undergo spontaneous deformation. Combating deformation is a high priority from the technological and design standpoint [2]. The use of modeling to determine the cause and degree of deformation which takes place can significantly shorten the time needed to begin production of a new product and select the necessary heat-treatment regime.

In the course of calculations performed for quenching and normalizing tubes, we obtained data on the distortions of the product (Fig. 5) and its residual stresses (Fig. 6). It was found that cooling in different media leads to different types
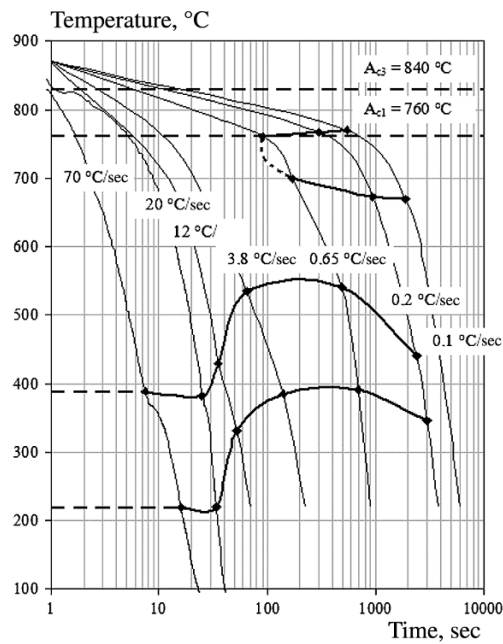
Fig. 3. Thermokinetic diagram of the decomposition of supercooled austenite in steel 26Kh1MFA cooled from $t = 880°C$.

TABLE 1. Chemical Composition of the Steels, wt.%[*]

Steel	Chemical element					
	C	Mn	Si	Cr	Mo	Ni
20MoCr_022C (ESI database)	0.22	0.56	0.30	0.56	0.44	0.15
26Kh1MFA	0.26	0.62	0.25	1.60	0.43	0.09
[*] The remainder is Fe.						

TABLE 2. Chemical Composition of the Alloys, wt.%[*]

Alloy	Chemical element							
	Mg	Si	Mn	Fe	Cu	Cr	Zn	Ti
AlMgSi (ESI database)	0.6–1.2	0.7–1.3	0.4–1.0	<0.5	<0.1	0.25	<0.2	<0.1
AD35	0.8–1.4	0.8–1.2	0.5–0.9	<0.5	<0.1	–	<0.2	<0.15
[*] The remainder is Al.								

of deformation. During *cooling in a sprayer*, the maximum change in the dimensions of the product is 0.5 mm for a wall-thickness of 8 mm. Thus, the magnification in the figure which depicts the calculated distortions of the tube was increased to 200 to clearly show the change in the product's shape (see Fig. 5*a*). Here, most of the deformation was concentrated at the edges of the tube and entailed bending of the edges inward.
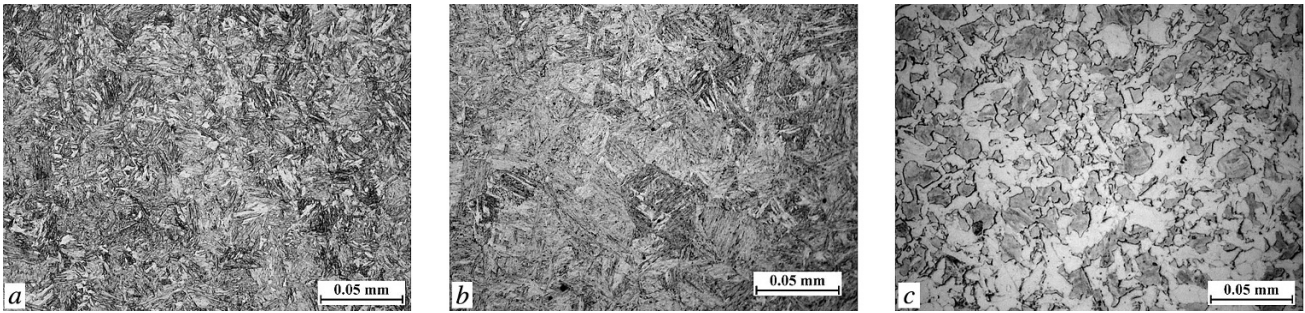
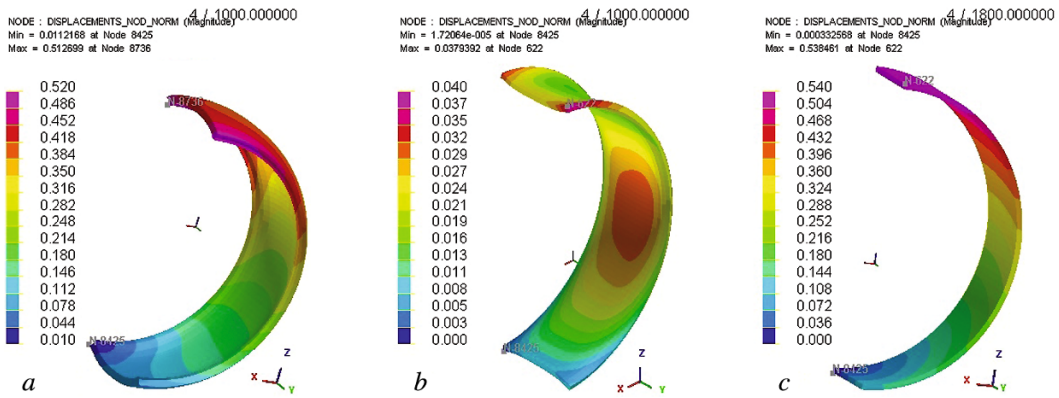Fig. 4. Structure of steel 26Kh1MFA after cooling at different rates from $t = 880°C$: *a*) water; *b*) oil; *c*) air.

Fig. 5. Calculated distortions of the pipe: *a*) quenching in the sprayer, ×200; *b*) quenching in oil, ×1000; *c*) normalization, ×200.
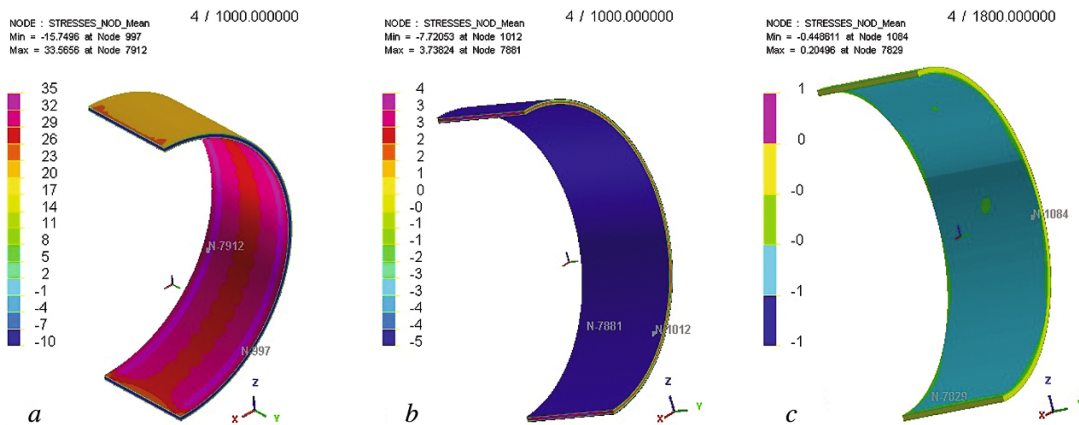

Fig. 6. Calculated residual stresses in the pipe: *a*) quenching in the sprayer; *b*) quenching in oil; *c*) normalization.

There was a different change in the shape of the tube when it was *quenched in oil*: the edges of the tube bent outward (see Fig. 5*b*). However, the largest change in the tube's dimensions was just 0.04 mm, which is an order less than in the case of quenching in a sprayer.

In contrast to the two cases described above, during *normalization* of the tube there was a uniform change in its shape over its entire length. Specifically, the tube assumed an oval form. The maximum displacements were 0.5 mm (see Fig. 5*c*).
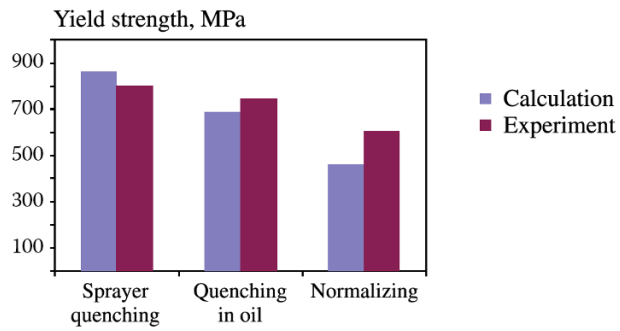
1015

Fig. 7. Comparison of experimental and calculated values of yield strength.
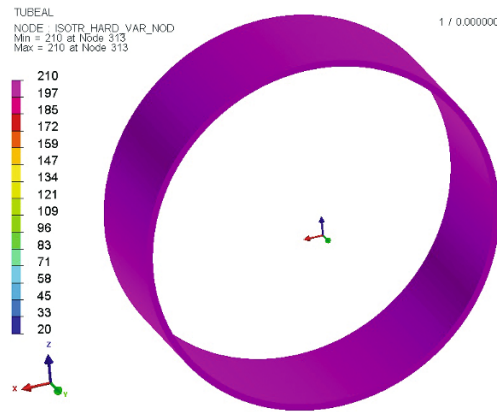

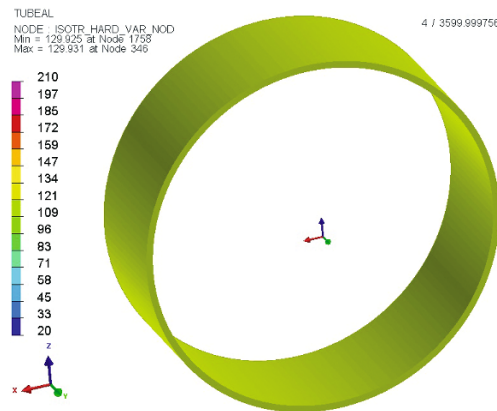Fig. 8. Initial yield strength.

Fig. 9. Calculated yield strength.

The formation of residual stresses in the tube also depends on the heating and cooling conditions. The tube with the highest tensile and compressive stresses (33.5 and 15.7 MPa, respectively) had a martensitic structure. The compressive stresses were localized at the center of the tube, while the tensile stresses were concentrated on its surface (Fig. 6a). In the case of the martensite-bainite structure. (Fig. 6b), the stresses decreased by an order of magnitude: the compressive stresses were at the level 8 MPa and the tensile stresses were at the level 4 MPa. The residual stresses were close to zero when the tube was cooled in air (Fig. 6c).

TABLE 3. Mechanical Properties of Steel 26Kh1MFA

HT regime	HV	HB	$\sigma_{0.2}$, MPa
Quenching in water	510	477	800
Quenching in oil	470	444	740
Normalization	390	363	600

Values of yield strength were also determined during the calculations. To evaluate yield strength in an actual material, we performed measurements of the Vickers hardness of specimens of steel 26Kh1MFA. It is known [3] there is a quantitative relationship between the hardness of ductile materials determined by the indentation method and other mechanical properties. The relationship between hardness on the one hand and ultimate strength and yield strength on the other hand is characterized by the following formulas:

$$\sigma_u = 3.3HB, \text{ MPa}; \tag{1}$$

$$\sigma_{0.2} = 1.7HB, \text{ MPa}. \tag{2}$$

Table 3 shows measured values of hardness and values of yield strength obtained with Eq. (2).

Figure 7 compares calculated and experimental values of the yield strength of the material after the use of different heat-treatment regimes. It is apparent that the two sets of values are very similar.

The difference in yield strength after quenching was on the order of 7%. This difference increased to 20% after normalization, which might be related to the formation of a more complex structure that included products of the decomposition of austenite I, II, and III. This development complicates calculation of the mechanical parameters. Considering all of these factors, however, it can be concluded that the results obtained from calculation of the mechanical properties in Visual Heat Treatment are adequate even in the presence of complex structures.

Calculations performed for the heat treatment of the aluminum tube showed the following. The alloy's initial structure in the database, which reflects its state after quenching and aging, was characterized by a yield strength of 210 MPa (Fig. 8).

During annealing of the tubular semifinished product at 370°C, the yield strength calculated in the program was 22 MPa. This result is related to the occurrence of annealing and recrystallization processes, as well as to "softening" of the elastic moduli at this temperature ($\approx 0.6T_{ml}$). Further cooling to room temperature was accompanied by an increase in yield strength to 130 MPa, which corresponds to the handbook data [4].

In light of the fact that both pure aluminum and its alloys have high thermal conductivity, that the cooling rate was low, and that no polymorphic transformations occurred in the pure aluminum, the same properties were obtained in the near-surface layers and at the middle of the semifinished product. This is apparent from the monochromatic contour of the images of the model (Fig. 9).

The heat treatment being discussed is usually an intermediate operation between hot and cold deformation and is designed to increase the ductility of semifinished products in order to be able to obtain the desired final shape. Annealing is accompanied by recrystallization processes that reduce dislocation density and form nondefective grains. The closely spaced fine particles of the strengthening phase (Mg_2Si) – which act as barriers to dislocations – undergo dissolution, which transfers alloying elements to the solid solution. The elements subsequently leave the solid solution during the coagulation of coarse particles that are spaced farther apart, and dislocations may be bent in the process (such as by the Orowan mechanism). This increases the mean free path and, thus, the degree of plastic deformation which takes place.

All of the above processes, which increase the ductility of the material, lead to a decrease in its strength characteristics. This decrease is manifest mainly as a reduction in yield strength.

Conclusion. The use of mathematical modeling makes it possible to select an appropriate heat-treatment regime in accordance with the required mechanical properties, the deformation which takes place, and the structural components of the alloy.

Comparison of the results of calculations in Visual Heat Treatment and experiments performed on steel 20KhMF showed that the data obtained on the distribution of the structural components is consistent with the thermokinetic diagram for the decomposition of supercooled austenite and the results obtained from metallographic studies.

Results on distortion and plastic strain were obtained above. It was shown that the formation of a predominantly martensitic structure in tubes of low-alloy steel leads to inward bending of the tube's edges and formation of the maximum amount of plastic strain. The edges also undergo bending in tubes with a martensite-bainite structure, but the bending is in the opposite direction. During normalization, distortion of the tube give it an oval shape. The residual stresses are close to zero in this case.

It was determined that the calculated level of the mechanical properties corresponds to the level determined empirically. The difference between the calculated and experimental values of yield strength for the martensitic structure and the martensite-bainite structure is small and amounts to just 7%.

The models that are part of the given software program are adequate for calculating the yield strength of aluminum alloys in the Al–Mg–Si system.

REFERENCES

1. M. A. Smirnov, V. M. Schastlivtsev, and L. G. Zhuravlev, *Principles of the Heat Treatment of Steel: Handbook*, Nauka i Tekhnologiya, Moscow (2002).
2. Yu. M. Lakhtin and A. G. Rakhshtadt (eds.), *Heat Treatment in Machine-Building: Handbook*, Mashinostroenie, Moscow (1980).
3. Yu. A. Geller and A. G. Rakhshtadt, *Materials Science. Methods of Analysis, Laboratory Assignments, and Problems*, Metallurgiya, Moscow (1984).
4. F. I. Kvasov and I. N. Fridlyander (eds.), *Commercial Aluminum Alloys*, Metallurgiya, Moscow (1984).